Journal of the Physical Society of Japan
Vol. 74, No. 7, July, 2005, pp. 1895–1898

Nonequilibrium Molecular Dynamics Simulation of Electric Conduction

Tatsuro YUGE*, Nobuyasu ITO[1†] and Akira SHIMIZU[‡]

Department of Basic Science, University of Tokyo, 3-8-1 Komaba, Meguro-ku, Tokyo 153-8902
[1]*Department of Applied Physics, School of Engineering, University of Tokyo, 7-3-1 Hongo, Bunkyo-ku, Tokyo 113-8656*

(Received April 11, 2005; accepted April 25, 2005)

We propose a realistic model for electric conduction, and study transport phenomena by molecular dynamics simulation. We observe that the system reaches a nonequilibrium steady state in the presence of an external electric field. The electrical conductivity is almost independent of the impurity distribution and the system size, and there is no long-time tail. The fluctuation–dissipation theorem and the Kramers–Kronig relation hold at all frequencies. These results show that this model has normal transport properties.

KEYWORDS: electric conduction, nonequilibrium molecular dynamics, complex admittance, Drude formula, fluctuation–dissipation theorem, long-time tail
DOI: 10.1143/JPSJ.74.1895

Electric conduction has been the central subject of nonequilibrium thermodynamics and statistical physics since Johnson[1)] experimentally discovered the fluctuation–dissipation theorem (FDT)[2,3)] relating the conductance and the equilibrium fluctuation of current. Despite long years of research after Johnson[1)] and Nyquist,[2)] there still remain many problems to be solved, including the long-time tail,[3)] response to nonmechanical forces,[4)] and a possible universal scaling relation of current fluctuations in nonequilibrium states.[5)] In particular, a simple and fundamental question is yet to be answered: Is there a statistical physics beyond the linear response theory?

One of the great difficulties in solving these problems is the difficulty in calculating nonequilibrium states theoretically. A promising approach seems to be computer simulations of nonequilibrium states. For heat conduction, it was recently shown, using nonequilibrium molecular dynamics (MD) simulation, that simple and feasible models show natural heat conduction.[6–8)] That is, basic models of interacting particles, including nonlinear lattices, hard particles, and Lennard-Jones systems, exhibit the Fourier-type heat conduction in three dimensions, although anomalous behaviors appear in lower dimensions.[6)] Note that momentum transfer is absent and the local equilibrium is well established in heat conduction,[6–8)] whereas momentum transfer is essential and the local equilibrium is sometimes destroyed in electric conduction.[9)] Despite these fundamental differences, the success of MD simulation of heat conduction encourages us to study electric conduction using MD simulation of a mechanical model.

In the present letter, we propose a new model of electric conduction, which has all the essential elements of real systems. The model is a genuine mechanical model, except for thermal walls (which simulate heat contact with a good sample holder) for heat carriers which we call phonons. Using MD simulation, we study nonequilibrium as well as equilibrium properties of the model, and show that all the results of the linear response theory are successfully reproduced at all frequencies. Although we assume a two-dimensional system in MD simulations, the long-time tail is absent. Rather surprisingly, the Drude formula holds well, although electron–electron and electron–phonon collisions take place more frequently than electron–impurity collisions.

Before constructing a model, let us summarize the essential elements in nonequilibrium steady states in electric conduction. A typical configuration of experiments on electric conduction is as follows. A uniform conductor is mounted on a large sample holder. Although the conductor is macroscopically uniform, it contains random impurities which violate the microscopic translational invariance and govern the conductivity σ at low temperature. When electric current I is induced by applying an external electric field E,[10)] energy is constantly supplied to the conductor, $W = IE$ per unit time. This energy is not dissipated into the environment by either electron–impurity (e–i) interactions, which are potential forces, or electron–electron (e–e) interactions because they conserve the total energy of the electron system. The supplied energy is transfered to the sample holder through the walls of the conductor as Joule heat. The rate of heat transfer equals W at steady states, wherein the temperature is higher than that before E is applied. To keep the temperature rise as small as possible (preferably, negligibly small), the sample holder is made of a material with a large heat capacity and good heat conduction. The heat flow in the conductor is mediated by electrons and phonons, while the heat flow across the walls of the conductor is mediated not by electrons but by phonons.[11)] Note that heat can be transfered outside the conductor *only through the walls*; it is impossible to 'teleport' heat from the center region of the conductor directly to the outside. Thus, electrons must transfer their energy to phonons in order to transfer heat to outside the conductor. Therefore, the electron–phonon (e–p) interactions and heat contact of phonons at the walls are essential to realize a nonequilibrium steady state. The e–p interactions also govern σ at high temperature. Note that these observations are also applicable to other transport processes such as the transport of neutral particles if terms such as electron, phonon and electric field are replaced by other applicable terms. For convenience, we use the terminology

*E-mail: yuge@ASone.c.u-tokyo.ac.jp
†E-mail: ito@ap.t.u-tokyo.ac.jp
‡E-mail: shmz@ASone.c.u-tokyo.ac.jp

of electric conduction throughout this paper.

We now propose a model which has all these essential elements. The system is composed of three types of classical particles, which we call electrons (with mass $m_{\rm el}$ and charge e), phonons, and impurities. At around room temperature, the number density $n_{\rm ph}$ of phonons is high, and hence the nonconservation of the phonon number seems irrelevant. Furthermore, the energy-momentum dispersion relations of phonons are complicated in real solids.[12] However, such complications seem unimportant when discussing the bare essentials of nonequilibrium states, although they will be important when discussing the properties of individual materials. Therefore, we here model the phonons as particles, whose number $N_{\rm ph}$ is conserved, with a parabolic dispersion relation with mass $m_{\rm ph}$. We assume that interactions among all particles, i.e., e–e, e–i and e–p interactions as well as p–p and p–i interactions, are present. The interaction potential between any two particles is taken as the Hertz type, represented by

$$V_{ij} = \begin{cases} U_{ij} d_{ij}^{5/2} & (d_{ij} > 0) \\ 0 & (d_{ij} \le 0), \end{cases} \tag{1}$$

where U_{ij} is a constant, $d_{ij} = R_i + R_j - |\boldsymbol{r}_i - \boldsymbol{r}_j|$ is the overlap of the potential ranges, R_i and R_j are the radii of the potential ranges ($R_{\rm el}$, $R_{\rm ph}$ and $R_{\rm imp}$ for an electron (e), phonon (p) and impurity (i), respectively), and $\boldsymbol{r}_i$ and $\boldsymbol{r}_j$ are the positions of the particle centers. We assume a two-dimensional classical system, the size of which is $L_x \times L_y$, although the model is applicable to any dimensions. There exists an external electric field E in the x-direction, which acts on only electrons, and the boundary condition in this direction is periodic. The boundaries in the y-direction are potential walls for the electrons (simulating the walls of the conductor), and thermal walls with temperature T for the phonons (simulating thermal contact with a good sample holder). The impurities are at rest and act as random potential. Note that this model is an almost purely mechanical model except for the thermal walls for the phonons.

We study transport properties of this model by MD simulation. We use Gear's fifth-order predictor–corrector method to solve the equations of motion. We take $m_{\rm el}$, $R_{\rm el}$, $k_{\rm B}T$ and e to be unity. The time-step width is fixed to be 10^{-3}, and we take $m_{\rm ph} = 1$, $R_{\rm ph} = R_{\rm imp} = 1$ and $U_{ij} = 4000$ (for all pairs of particles). The initial positions of particles are so arranged as not to contact each other, and the initial velocities of particles are given by the Maxwell distribution. The thermal walls reflect phonons back, with random velocities whose probability distribution function is given by

$$f(\boldsymbol{v}) = \frac{1}{\sqrt{2\pi}} \left(\frac{m_{\rm ph}}{k_{\rm B}T} \right)^{3/2} |v_y| \exp\left(-\frac{m_{\rm ph} v^2}{2k_{\rm B}T} \right). \tag{2}$$

First, we check whether the system reaches a nonequilibrium steady state in the presence of E. We define the electric current in the x-direction at time t as

$$I(t) = e n_{\rm el} L_y v_{\rm el}^x(t), \tag{3}$$

where $n_{\rm el} = N_{\rm el}/L_x L_y$ is the density of the electrons, $v_{\rm el}^x(t) = \sum_{i=1}^{N_{\rm el}} v_i^x(t)/N_{\rm el}$ is the average velocity in the x-direction per electron, $N_{\rm el}$ is the total number of the electrons in the system and v_i^x is the velocity of each electron in the x-direction. Figure 1 depicts a typical result of the time evolution of $I(t)$. We can see that $I(t)$ increases from $I(0) \simeq 0$ and then fluctuates around the time-averaged value for $t \gtrsim 100$. The inset of Fig. 1 shows the time-averaged value, which is almost independent of the upper limit $\mathcal{T}$ of the time range. Therefore, a nonequilibrium steady state is realized.

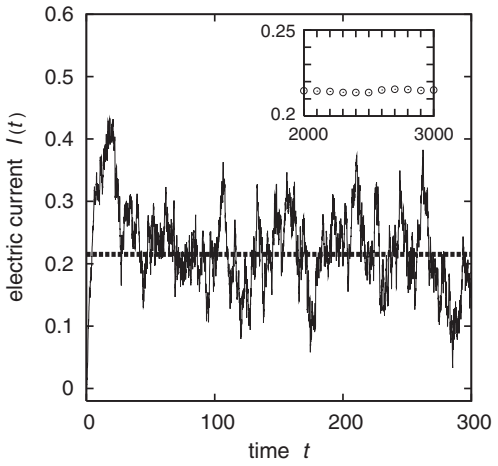

Fig. 1. Electric current $I(t)$ as a function of time for a typical initial condition. The parameters are $L_x = 480$, $L_y = 24$, $N_{\rm el} = 300$, $N_{\rm ph} = 90$, $N_{\rm imp} = 120$, and $E = 0.10$. The broken line shows the time-averaged value of $I(t)$. The inset shows the mean values of $I(t)$ averaged over the time range $[500, \mathcal{T}]$ as a function of $\mathcal{T}$.

Next, we examine the dependence of the electrical conductivity $\sigma = \langle I \rangle / E L_y$ on the impurity distribution, where $\langle I \rangle$ denotes the time-averaged value of $I(t)$. We calculate $\langle I \rangle$ for five distributions of impurities. The results are plotted in Fig. 2. It is seen that the values of $\langle I \rangle$ are almost the same among the five distributions for each value of E, i.e., σ is almost independent of the impurity distribution.

The solid line in Fig. 2 shows that there exists a region of linear response for $E \lesssim 0.03$, whereas the response becomes nonlinear for larger E. We can roughly explain this as

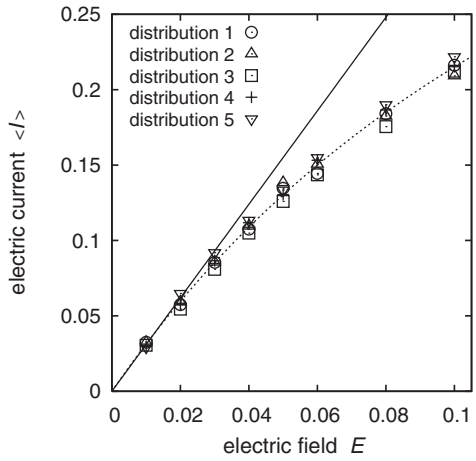

Fig. 2. Time-averaged electric current for various impurity distributions, plotted against an external electric field E. The values of parameters are the same as those in Fig. 1. The solid line is a straight line obtained from data for small E, and indicates a linear response. The broken line represents $\sigma(E) E L_y$, where $\sigma(E)$ is given by eq. (4).

follows. If we assume the Drude formula, σ is proportional to a certain relaxation time τ. Since U_{ij}'s are taken to be quite large, V_{ij} may be regarded as a hard core potential. Hence, τ may be roughly estimated as $\tau \simeq l/v_{\rm el}$, where l is the mean distance between scatterers, independent of E. An electron is accelerated by E, and its velocity $v_{\rm el}$ increases to $v_{\rm el}(E) \simeq v_{\rm el}(0) + eE\tau(E)/m_{\rm el}$ just before the collision, which is approximated by $v_{\rm el}(0) + eE\tau(0)/m_{\rm el}$ to the first order in E. Thus, the dependence of σ on E is expressed as

$$\sigma(E) \simeq \frac{\tau(E)}{\tau(0)}\sigma(0) \simeq \frac{v_{\rm el}(0)}{v_{\rm el}(0) + eE\tau(0)/m_{\rm el}}\sigma(0). \qquad (4)$$

The broken line in Fig. 2 represents $\sigma(E)EL_y$, where $\sigma(E)$ is given by eq. (4) and $v_{\rm el}(0) \simeq 1.4$ (which is estimated from $\langle m_{\rm el} v_{\rm el}(0)^2/2\rangle = k_{\rm B}T$), whereas the fitting parameters are $\sigma(0) \simeq 0.14$ and $\tau(0) \simeq 7.6$. This value of $\tau(0)$ is comparable to $l/v_{\rm el}(0) \simeq 5.3$ if we put $l \simeq 1/n_{\rm scatt}^{1/2} \simeq 7.4$, where $n_{\rm scatt} = (N_{\rm ph} + N_{\rm imp})/L_xL_y$ is the density of scatterers.

We also study the system-size dependence of σ. We calculate $\langle I\rangle$ for $L_x = 320$, 480 and 640 while keeping L_y and the densities constant ($L_y = 24$, $n_{\rm el} \simeq 0.026$, $n_{\rm ph} \simeq 0.0078$ and $n_{\rm imp} \simeq 0.010$). Figure 3 shows the result. It is seen that $\langle I\rangle$, and thus σ, is almost independent of the system size.

Next, we investigate the complex admittance $Y(\omega) = \widetilde{I}(\omega)/\widetilde{E}(\omega)L_x$ when the system is in an AC electric field $E(t) = E_0\sin(\omega t)$. Here, $\widetilde{\ }$ denotes the Fourier transform, and $E_0 = 0.020$ (which corresponds to the linear response region). We show the results in Fig. 4. Both the real and imaginary parts are well fitted by the Drude formula,

$$\mathrm{Re}[Y(\omega)] = \frac{Y(0)}{1 + (\tau\omega)^2}, \qquad (5)$$

$$\mathrm{Im}[Y(\omega)] = \frac{Y(0)\tau\omega}{1 + (\tau\omega)^2}, \qquad (6)$$

where $Y(0) \simeq 0.0067$ and $\tau \simeq 5.3$. [These values are comparable to those obtained from eq. (4) at $E = 0.020$.] Therefore, the Kramers–Kronig relation holds for this model. Recall that the Drude model is very simple because multiscatterings and many-body interactions are not taken account. On the other hand, our model does include such effects. In spite of these differences, the Drude formula seems to be valid in our model. This is rather surprising, and our model should provide us with a key to understanding why the Drude formula is widely valid for real systems.

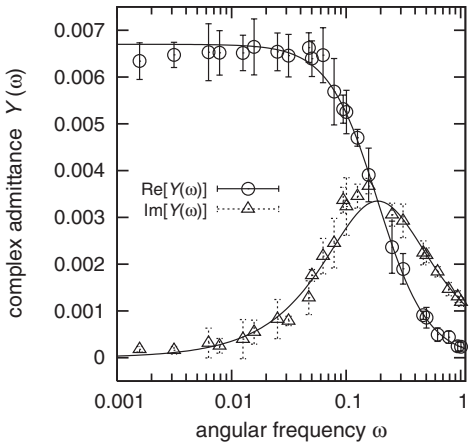

Fig. 4. Complex admittance plotted against angular frequency. The values of parameters are the same as those in Fig. 1. Circles and triangles indicate the real and imaginary parts of the admittance, respectively. Data points are the mean values, whereas the error bars indicate the rms, over five distributions of impurities. The solid lines show the Drude formula.

We now study whether FDT holds for our model. FDT for a classical electric conduction system is expressed as

$$g_I(\omega) = 2k_{\rm B}T\,\mathrm{Re}[Y(\omega)], \qquad (7)$$

where $g_I(\omega)$ is the spectral intensity of electric current in the equilibrium state at $E = 0$, and $Y(\omega)$ is the complex admittance plotted in Fig. 4. In Fig. 5, we compare the left-hand side (LHS) and the right-hand side (RHS) of eq. (7). We see that the LHS and RHS agree within the limits of the error bars. Hence, FDT holds for this model. Although the error bars for the LHS at low frequencies are large, we expect that they would become smaller if the number of averaging samples were greatly increased, and/or higher dimensions were adopted.

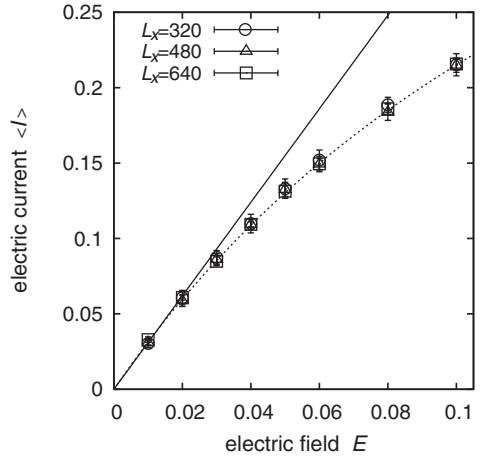

Fig. 3. Time-averaged electric current for various system sizes, plotted against an external electric field E. Circles, triangles and squares are for $L_x = 320$, 480 and 640, respectively. Data points are the mean values, whereas the error bars indicate the rms, over five distributions of impurities. The solid and broken lines are the same as those in Fig. 2.

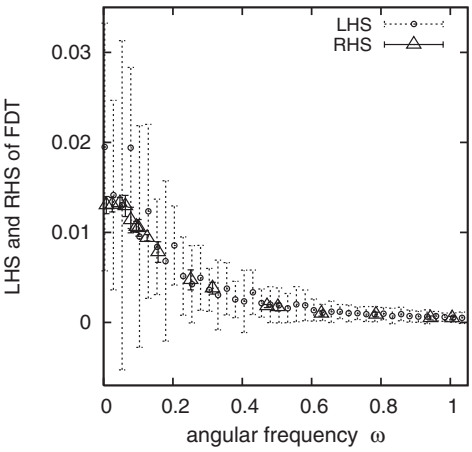

Fig. 5. LHS (circles) and RHS (triangles) of FDT, eq. (7), versus angular frequency. The values of parameters are the same as those in Fig. 1. Data points are the mean values, whereas the error bars indicate the rms, over 46 and five distributions of impurities for LHS and RHS, respectively.

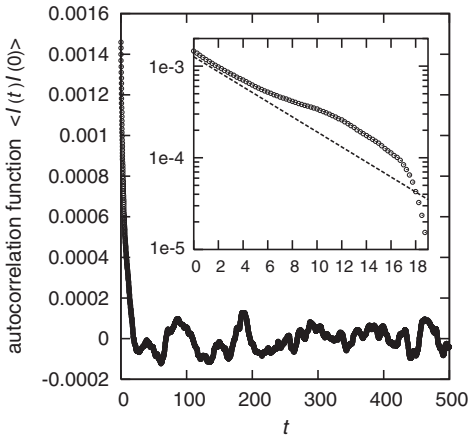

Fig. 6. Autocorrelation function of electric current. The values of parameters are the same as those in Fig. 1. The inset is a magnified plot for small t. The broken line indicates the inverse-Fourier transform of RHS of eq. (7), assuming the Drude formula [eq. (5)], and is proportional to $e^{-t/\tau}$.

Finally, we investigate the long-time tail, by calculating the autocorrelation function of electric current $\langle I(t)I(0)\rangle$ at equilibrium. The result is shown in Fig. 6. It is seen that $\langle I(t)I(0)\rangle$ decays at the same rate as or faster than $e^{-t/\tau}$, where τ is the same as that in eqs. (5) and (6). Thus, there is no long-time tail in this model. This property has already been reflected in the result that σ is almost independent of the system size (Fig. 3) and that the spectral intensity of electric current converges as $\omega \to 0$ (Fig. 5). In other models, the autocorrelation functions have long-time tails,[3,6,7,13–15] which results in logarithmic divergence (with the system size) of the heat conductivity in two-dimensional systems.[6,7,15] The absence of the long-time tail in the present model may be interpreted as being due to scatterings by impurities and phonons introducing a natural cut-off length.

Furthermore, if we assume the Drude formula, eq. (5), we can calculate the inverse-Fourier transform of the RHS of eq. (7) as

$$\frac{k_B T Y(0)}{\tau} e^{-|t|/\tau}, \tag{8}$$

which is plotted in the inset of Fig. 6 as the broken line. For small t, it agrees fairly well with $\langle I(t)I(0)\rangle$, which is the inverse-Fourier transform of the LHS of FDT [i.e., $g_I(\omega)$]. This also supports the validity of FDT in our model.

In summary, we have proposed a realistic model for electric conduction. The model is a two-dimensional classical system composed of electrons, phonons and impurities, in which an external electric field is imposed. We have studied the electric transport properties of this model by MD simulation. We have observed that the system reaches a nonequilibrium steady state, and that the electrical conductivity has almost no dependence on the impurity distribution or the system size. The complex admittance satisfies FDT at all frequencies, and is well fitted by the Drude formula, satisfying the Kramers–Kronig relation. Furthermore, the long-time tail, and thus the logarithmic divergence of the conductivity, is absent in spite of the low dimensionality. These results show that this model has normal transport properties. We thus believe that this model will become a good framework for studying nonequilibrium statistical mechanics beyond the linear response theory. We also expect that this model will help us to gain some ideas for research into nanometer-scale devices.

Acknowledgment

We thank S. Yukawa for helpful discussion.

1) J. B. Johnson: Phys. Rev. **32** (1928) 97.
2) H. Nyquist: Phys. Rev. **32** (1928) 110.
3) L. E. Reichl: *A Modern Course in Statistical Physics* (University of Texas Press, Austin, TX, 1980).
4) A. Shimizu and H. Kato: in *Low-Dimensional Systems—Interactions and Transport Properties*, ed. T. Brandes (Springer, Berlin, 2000) p. 3; A. Shimizu and H. Kato: cond-mat/9911333.
5) A. Shimizu, M. Ueda and H. Sakaki: *Proc. 4th Int. Symp. Foundations of Quantum Mechanics, Tokyo, 1991* (Publ. Office, JJAP, Tokyo, 1993) JJAP Series No. 9, p. 189.
6) T. Shimada, T. Murakami, S. Yukawa and N. Ito: J. Phys. Soc. Jpn. **69** (2000) 3150.
7) T. Murakami, T. Shimada, S. Yukawa and N. Ito: J. Phys. Soc. Jpn. **72** (2003) 1049.
8) F. Ogushi, S. Yukawa and N. Ito: J. Phys. Soc. Jpn. **74** (2005) 827.
9) A. Shimizu and M. Ueda: Phys. Rev. Lett. **69** (1992) 1403.
10) Although I is generally induced not by E but by $\nabla\mu$, the gradient of the (electro) chemical potential μ, we here assume a uniform system, for which $E = \nabla\mu/e$, as discussed in ref. 4.
11) Although electromagnetic fields and some other excitations (which are localized around the walls) may also play some roles, phonons seem to have the dominant role.
12) For example, the dispersion relation of acoustic phonons is linear at small momentum and nonlinear at higher momentum. Optical phonons have more complicated dispersion relations.
13) B. J. Alder and T. E. Wanwright: Phys. Rev. A **1** (1970) 18.
14) J. R. Dorfman and E. D. G. Cohen: Phys. Rev. A **12** (1975) 292.
15) S. Lepri, R. Livi and A. Politi: Phys. Rep. **377** (2003) 1.